The Atmosphere of Mars and Optical Communications

J. Annis
Communications Systems Research Section

The effects of the Martian atmosphere on an optical communication link are analyzed using Mariner 9, Viking Orbiter, and Viking Lander data. Clouds are found to have minimal effect because of their scarcity and thinness. Dust (from dust storms) has the dominant impact on opacity. However, periods of reduced visibility are infrequent and more closely resemble the effects of thin clouds on the Earth. A simple argument is presented which suggests that the Martian atmosphere has fewer turbulence-related effects (i.e., Mars has better resolution, lower image wander, and less scintillation) than the best of the Earth's ground-based locations.

I. Introduction

Optical communication links have been proposed for the Mars Rover. These communication systems have the high data rates and low mass, volume, and power consumption that the Rover requires. However, they face environmental problems that are different from those for radio systems, and these problems have never been evaluated for Mars and its atmosphere. This article will discuss the atmospheric effects that influence an optical communication system and will survey those effects in relation to the Martian atmosphere.

II. Optical Communications

Optical communication links are designed to operate near visible wavelengths (although they can also be in the infrared). The doubled Nd:YAG laser currently under consideration lases at 0.53 μm. This wavelength allows an exploration of the effects of the Martian atmosphere on an optical communication link using currently available data, as all the past planetary images were taken near this wavelength. In particular, the Viking Orbiters' images were at 0.44 μm to 0.59 μm and the Viking Landers' at 0.67 μm and 0.59 μm.

The two major effects of an atmosphere on an optical communication link are attenuation and scintillation [9]. Attenuation is caused by absorption and scattering due to both air molecules and aerosols. Optical depth, τ, is a measure of attenuation over the entire path length, here taken to be the distance from the ground to space. Optical depth increases as the line of sight moves down toward the horizon, increasing the path length. The power received, P_r, is the power transmitted, P_t, multiplied by the attenuation: $P_r = P_t e^{-\tau}$. An optical depth of 1 attenuates a signal by 63 percent. For comparison, a clear night on Earth has an optical depth of $\approx$0.2. The effect of attenuation is to reduce the visibility of the link.

Scintillation is caused by turbulence-induced spatial and temporal refractive index variations. Refractive index variations also cause the wavefront distortions that determine

resolution and image wander. The effect of scintillation is to increase the bit error rate. Resolution and image wander affect beam-pointing accuracy.

There may be some concern that aerosol dust affects resolution on Mars. There are really a number of problems involved in that concern. The laser beam from the surface may suffer an increased beam divergence due to the aerosols, or the laser beacon/illuminated Earth's image may be so far underresolved that pointing the laser is difficult. Both of these issues have been examined experimentally. Doubled Nd:YAG lasers fired through terrestrial fog with optical depths of 10 or greater suffered no increased beam divergence [8]. The same experiments found an increase in the apparent angle of the source (say, the Earth) by a factor of 4 at $\tau \approx 2$. This does not seem to pose a problem, as the typical optical depth is more like 0.5 and the base resolution of the atmosphere is high (see Section V). Comparison of fog with dust is justified because both are primarily Mie scatterers. This aspect of the dust, as well as a new problem that this brings, will be examined next.

Martian aerosol dust behaves as a Mie scatterer, except that it has a tendency to scatter more at high angles than does a Mie scatterer [6]. Mie scattering is characterized by large amounts of forward scattering. A receiver with a wide enough field of view would see three concentric circles: the direct (but attenuated by the optical depth) beam, the multiple forward-scattered photons, and the diffused photons (see Fig. 1, based on a figure in [5]). The light from both of the last two circles comes from the attenuation of the direct beam. It is possible for the multiple forward-scattered light, which has a size on the order of 2 degrees, to overwhelm the direct beam. While this does not concern a link looking at a laser fired through an aerosol (it just receives more photons than it should), the ability of a link to pick out the beacon/Earth might be in jeopardy. If the forward component dominated, the link would see a blur with a size of about 2 degrees. However, just by energy conservation, the scattered component cannot even equal the direct beam intensity until $\tau \approx 0.7$ ($e^{-0.7} \approx 0.5$), and experiments show that this does not occur until an optical depth of 15 [5]. At optical depths of 1 this does not seem to be a substantial concern.

III. The Atmosphere

On Mars, scattering by atmospheric molecules is negligible ($\tau \approx 0.002$), mainly because the atmosphere is extremely thin. Molecular absorption is also unimportant outside of a few deep absorption bands. This is also the case on Earth, where absorption features have been extensively tabulated between 0.4 μm and 10.0 μm. The locations and relative strengths of the Martian atmospheric absorptions are the same as those of the Earth's atmosphere to a first approximation, because most of the same gases appear in about the same proportions in each. On Mars, CO_2 will have relatively stronger lines and H_2O relatively weaker, but the only major addition, CO, has no absorption lines below 2.3 μm. These lines are easily avoided. Overall, there will be a pronounced decrease in the strength of the atmospheric absorption lines on Mars as a result of the thin atmosphere.

IV. The Aerosols

The major attenuators on Mars are the aerosol scatterers: clouds, fog, haze, and dust. The global and local properties of the attenuators have been studied using Mariner 9, Viking Orbiter, and Viking Lander data. Orbiter data are down-looking images that allow cloud type, cloud distribution, and optical depth to be determined. The Viking Lander data are up-looking images of the Sun and Phobos that allow precise optical depth measurements.

A. Combined Effects

The optical depth of the Martian atmosphere and its variation over a season were examined by Thorpe [10] using Viking Orbiter images taken during northern summer/southern winter. The measurements were made in three regions: the Viking Lander 1 region (northern equatorial latitudes); the Smooth Plains (northern equatorial region and mid-latitudes); and the Old Terrain (southern mid-latitudes). The Viking Lander 1 region results are consistent with those from the lander itself. The other two regions have optical depth histories that are similar to that of the Lander 1 site: $\tau \approx 0.2$–0.3, with short excursions to 0.6. These probably represent the thicker hazes that Kahn's statistics (see Subsection C) say should be in at least one place in these regions 20 to 30 percent of the time.

The Viking Landers returned optical depth data at two locations on the surface of Mars for almost a Martian year. The history at 22 degrees N, Viking 1 in the northern equatorial latitudes, is shown in Fig. 2. The history at 48 degrees N, Viking 2 in the northern mid-latitudes, is shown in Fig. 3. (Both figures are from [6], and both express the time coordinate in terms of sol number, i.e., the number of Martian solar days from touchdown.) The global dust storms are the two excursions to high optical depths. Other than the dust storm, the largest effect seen was at Viking Lander 2, where for less than a day the optical depth grew larger than 1, reaching 2.8 (see Fig. 4, derived from [11]). This was identified as a cold front associated with the north polar hood passing the lander [11]. It was not seen at the other lander farther south. For comparison, a terrestrial cumulus cloud has an optical depth of $\approx$ 6–200. Viking 1 found a background haze of $\tau \approx 0.3$, while Viking 2 found a similar haze of $\tau \approx 0.5$. Pollack *et al.* [6], [7] identify this as 5 μm dust particles from local dust storms

suspended in the atmosphere. Both landers also saw a diurnal variation in τ of about 0.2 (see Fig. 5, derived from [6]) during the Martian summer. As this additional optical depth appears before sunrise and disappears around noon, it has been identified with (H_2O) fog.

B. Dust

Local dust storms were seen to occur almost entirely in two locations: at the edge of the retreating southern polar cap and in the low-latitude regions of the southern hemisphere [7]. The coverage of the southern hemisphere was more complete than that of the northern hemisphere, however. The low-latitude storms occur mostly when Mars is at perihelion. Local dust storms last on the order of a day.

Global dust storms can last for 70 days. They typically happen once a Martian year, in the southern hemisphere's late spring to summer. The Martian year that the Viking Landers spent on Mars was particularly bad; there were two global dust storms. The more southerly lander, Viking 1, saw higher optical depths measuring $\tau = 2.7$, and $\tau = 3.7$ for the storms. Pollack *et al.* [7] estimate an upper limit on the dust storms of $\tau = 3.2$ and $\tau = 9$, respectively. These storms are apparently caused by solar heating of the atmosphere acting on local dust storms in a feedback mechanism. They feature high winds and blowing dust, so it is doubtful that any communication link would be used during a storm.

C. Clouds

The Viking Orbiters and Mariner 9 provided us with 58,000 images of Mars. Of these, 2.4 percent had some form of cloud or fog, and 28 percent had visible haze. These images have been cataloged and the cloud occurrence statistics tabulated by Kahn [4]. Table 1 shows a simplified version of this table. Although this grossly oversimplifies the weather patterns of the planet, the statistics can help sketch out the large patterns. The statistics are broken up by cloud type, season, and latitude range. Each entry should be read as "the probability of finding at least one cloud of this type in this latitude range during this season." Not surprisingly, there is a distinct seasonal dependence as well as a latitude dependence. Not shown are a longitude dependence and a time-of-day dependence [3], [4]. Some Martian clouds form at dawn and burn off rapidly, and others form only in the midday.

In general terms the occurrence patterns of Martian clouds may be described as follows, paraphrased from Kahn [4]. The northern hemisphere is, in general, more cloudy than the southern hemisphere in corresponding seasons. Clouds generally form more easily in mid-latitudes than in the equatorial regions, and more easily still in the polar regions. Clouds are relatively abundant during northern spring and summer at mid-latitudes; in the southern hemisphere mid-latitudes the situation is complicated by atmospheric dust. Thick H_2O clouds are not found at high latitudes during mid-to-late autumn or winter in either hemisphere, nor are they found in southern mid-latitudes during early winter. Overall, the optical thickness of Martian clouds is $\approx$0.05–3.0, a figure closer to terrestrial cirrus clouds ($\tau \approx 0.3$–3.5) than to stratus clouds ($\tau \approx 6$–80) or cumulus clouds ($\tau \approx 5$–200) [9].

Widespread, optically thick clouds occur in three regions [1]. The polar regions have a seasonally dependent bank of H_2O and CO_2 clouds as well as hazes around their perimeters, known as polar hoods. It seems the hazes have optical thicknesses on the order of 1, while clouds are thicker [2]. The second region is the Tharsis Bulge. Here, on the northwestern flanks of the four large volcanoes, optically thick clouds ($\tau \geq 1$) are found perhaps 25 percent of the time. These clouds are caused by wind moving over the volcanoes. The third area of widespread clouds is the plateau region south of the western end of the Marineris valley, where a field of cellular clouds is a daily occurrence during the summer.

Isolated clouds are often found in other locations [1], [3], [4]. The most common type is the lee cloud, which can be optically thick. These fairly small clouds form downwind of craters, in the same way as the Tharsis Volcano clouds. When they occur, these clouds are numerous enough to be used to map out wind patterns on a regional scale. Wave clouds are much like lee clouds in thickness and in occurrence rates but are not associated with a ground obstacle. Optically thin cirrus clouds are relatively common. These clouds, probably CO_2, are widespread when they occur but have optical thicknesses of only $\approx$0.05. Hazes are also noted by Kahn [4]. It is not clear if they are dust or ice, but they can have optical depths ≥ 1.

D. Fog

Optically thick fog was seen in some crater bottoms and in the Marineris valley, particularly in the Labyrinthus Noctus [1]. Terrestrial fogs are about 150 meters thick and have optical depths of $\approx$3. Although the hourly coverage was not good, the fog seems to burn off in the afternoon. The fog seen by the Viking Landers was thin, about $\tau = 0.2$, and apparently would not have been seen by the orbiters. Fog occurs mostly in the spring and summer, and mostly in the southern hemisphere.

V. Turbulence

The size of the turbulence-induced effects is hard to determine from Viking data. The images give practically no information, as the expected effects are below the resolution limits of the imagers (the 0.12-degree diodes on the landers were

stepped in 0.04-degree intervals; on Earth bad resolution is 0.03 degree). However, the theories of index-of-refraction effects developed for the Earth's atmosphere can be applied to the case of the Martian atmosphere. An order-of-magnitude argument using these theories is presented here.

The distortion capabilities of turbulence are directly related to the size of the mean square fluctuations of the index of refraction, C_N. In turn, C_N is directly related to the size of the mean square fluctuations of temperature, C_T, with the relation expressed as:

$$C_N = \text{const} \frac{P}{T^2} C_T$$

where T is the temperature and P is the pressure. The ratio of the fluctuations on Mars to those on Earth is then:

$$\frac{C_{N,\,\text{Mars}}}{C_{N,\,\text{Earth}}} = \frac{P_{\text{Mars}}}{P_{\text{Earth}}} \left(\frac{T_{\text{Earth}}}{T_{\text{Mars}}}\right)^2 \frac{C_{T,\,\text{Mars}}}{C_{T,\,\text{Earth}}}$$

The first factor on the right is on the order one hundredth, and the second factor on the right is on the order of 1. It seems very unlikely that the temperature fluctuations on Mars are one hundred times larger than those on Earth (bear in mind that these are short time scale variations). More likely is that the index of variation fluctuations in the Martian atmosphere is one hundred times smaller than that of the Earth's atmosphere. This suggests that the average location on Mars has a view of an optical communication link that is one hundred times more stable than the average location on Earth.

VI. Conclusions

Mars's weather may be simpler than the Earth's weather, but it is still a very complex system. By making sweeping generalizations, the overall results can be shown in Table 2, which compares Mars and the Earth. In general, optically thick clouds and fog are fairly rare on Mars. Aerosol dust is always present and is the main source of atmospheric opacity. The great dust storms are the cause of the highest opacity, $\tau \approx 10$. Attenuation losses due to clouds, fog, and dust seem modest. However, such visibility still corresponds to thin clouds on the Earth. The turbulence-induced effects, such as scintillation and wavefront distortion, should be less of a problem on Mars than on Earth. Aerosol dust may have some impact on resolution, but it should not be great. More than likely, the surface of Mars has routinely better visibility than Earth's best locations both in terms of resolution and in terms of lack of scintillation and image movement. It certainly has clear weather much more often.

References

[1] G. Briggs, K. Klaasen, T. Thorpe, J. Wellman, and W. Baum, "Martian Dynamical Phenomena During June-November 1976: Viking Orbiter Results," *J. Geophys. Res.*, vol. 82, pp. 4121-4149, 1977.

[2] P. R. Christensen and R. W. Zurek, "Martian North Polar Hazes and Surface Ice: Results from the Viking Survey/Completion Mission," *J. Geophys. Res.*, vol. 89, pp. 4587-4596, 1984.

[3] R. G. French, P. J. Gierasch, B. D. Popp, and R. J. Yerdon, "Global Patterns in Cloud Forms on Mars," *Icarus*, vol. 45, pp. 468-493, 1981.

[4] R. Kahn, "The Spatial and Seasonal Distribution of Martian Clouds and Some Meteorological Implications," *J. Geophys. Res.*, vol. 89, pp. 6671-6688, 1984.

[5] G. C. Mooradian, M. Geller, L. B. Stolts, D. H. Stephens, and R. A. Krautwald, "Blue-Green Propagation Through Fog," *Applied Optics*, vol. 18, pp. 429-441, 1979.

[6] J. B. Pollack, D. Colburn, R. Kahn, J. Hunter, W. Van Camp, C. E. Carlston, and M. R. Wolf, "Properties of Aerosols in the Martian Atmosphere, as Inferred from Viking Lander Imaging Data," *J. Geophys. Res.*, vol. 82, pp. 4479-4496, 1977.

[7] J. B. Pollack, D. S. Colburn, F. M. Flasar, R. Kahn, C. E. Carlston, and D. Pidek, "Properties and Effects of Dust Particles Suspended in the Martian Atmosphere," *J. Geophys. Res.*, vol. 84, pp. 2929–2945, 1979.

[8] W. S. Ross, W. P. Jaeger, J. Nakai, T. T. Nguyen, and J. H. Shapiro, "Atmospheric Optical Propagation: An Integrated Approach," *Applied Optics*, vol. 21, pp. 775–785, 1982.

[9] The Technical Cooperation Program, "The Application of Optical Space Communication to the Military Communications Requirements: A User's Guide," presented at the Laser Communication Workshop, Technical Panel STP-6, Space Communications, Salisbury, Australia, October 29 to November 2, 1984.

[10] T. Thorpe, "Viking Orbiter Observations of Atmospheric Opacity During July–November 1976," *J. Geophys. Res.*, vol. 82, pp. 4151–4159, 1977.

[11] J. E. Tillman, R. M. Henry, and S. L. Hess, "Frontal Systems During Passage of the Martian North Polar Hood over the Viking Lander 2 Site Prior to the First 1977 Dust Storm," *J. Geophys. Res.*, vol. 84, pp. 2947–2955, 1979.

Table 1. Martian cloud occurrence statistics

Season	Latitude range	Occurrence probabilities (%)			
		Thin clouds ($\tau < 1$)	Thick clouds ($\tau \geq 1$)	Fog	Haze ($\tau \geq 1$)
Northern spring	Polar	9	24	0	22
	Mid-latitudes	6	10	0	10
	Equatorial	6	6	0	8
Southern fall	Equatorial	5	16	5	7
	Mid-latitudes	3	19	3	8
	Polar	26	59	8	7
Northern summer	Polar	31	24	7	27
	Mid-latitudes	11	10	0	13
	Equatorial	10	16	3	24
Southern winter	Equatorial	8	12	3	10
	Mid-latitudes	19	23	17	15
	Polar	4	4	4	0
Northern fall	Polar	12	1	0	60
	Mid-latitudes	11	6	0	38
	Equatorial	1	1	0	25
Southern spring	Equatorial	6	9	5	33
	Mid-latitudes	10	27	18	54
	Polar	28	7	33	67
Northern winter	Polar	7	0	0	0
	Mid-latitudes	10	17	0	32
	Equatorial	2	2	2	13
Southern summer	Equatorial	17	7	6	19
	Mid-latitudes	19	26	28	21
	Polar	33	18	21	30

Table 2. Comparison of Earth and Mars generalized weather patterns

Atmospheric condition	Earth		Mars	
	Typical optical depth	Distribution	Typical optical depth	Distribution
Atmospheric absorption and Rayleigh scattering	0.2	Everywhere	0.002	Everywhere
Aerosol dust	–	–	0.5	Everywhere
Dust storms	–	–	10.0	Southern hemisphere or global
Fog	≈3	Many places	≈1.0	Morning; crater bottoms and valleys
			0.2	Morning; everywhere?
Clouds H_2O	≈5	50% cloud cover	≈1.0	Winter polar; isolated; clouds behind high places
Clouds CO_2	–	–	≈0.001	Many places
			≈1.0	Winter polar regions

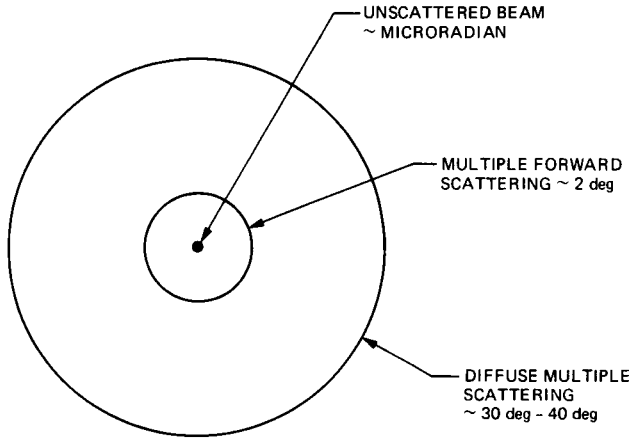

Fig. 1. Schematic representation of laser angular brightness distribution due to Mie scattering in optically thick regions

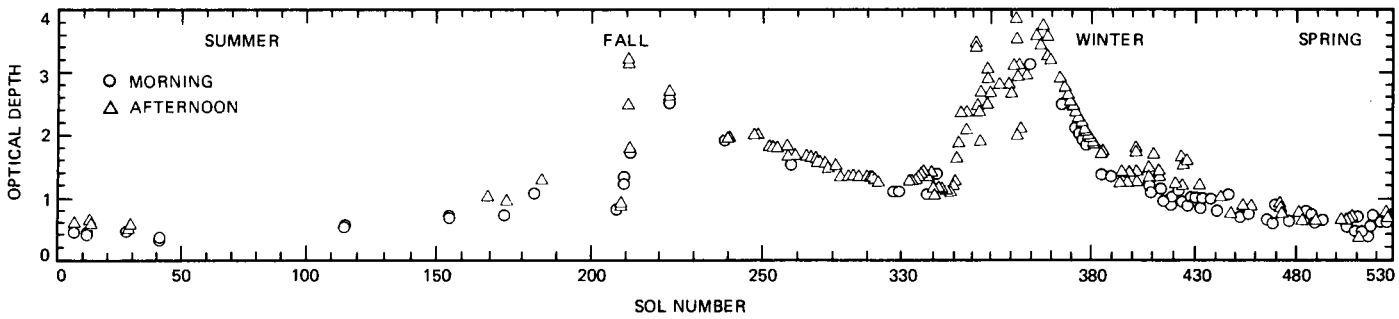

Fig. 2. Optical depth at the Viking Lander 1 site as a function of time

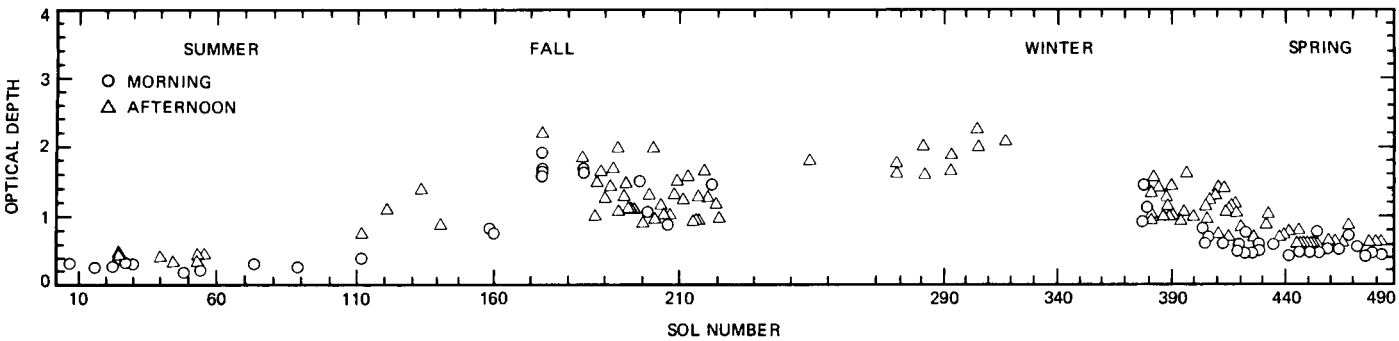

Fig. 3. Optical depth at the Viking Lander 2 site as a function of time (sol 0 here is equivalent to sol 44 for the Viking Lander 1)

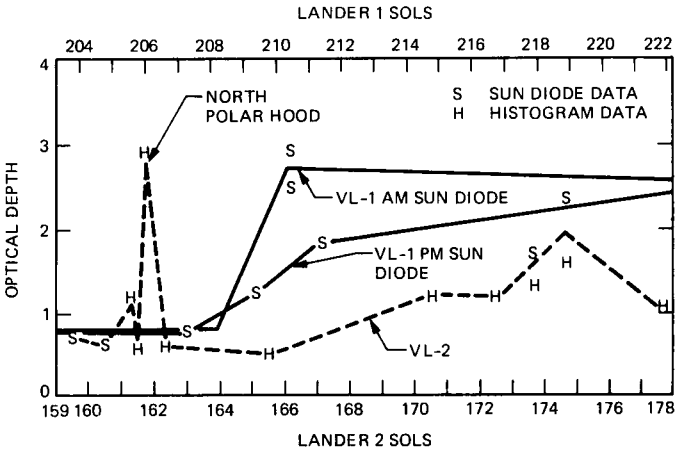

Fig. 4. Optical depth data from both landers (histogram data are derived from analysis of images, while the sun diode data are derived from imaging the sun)

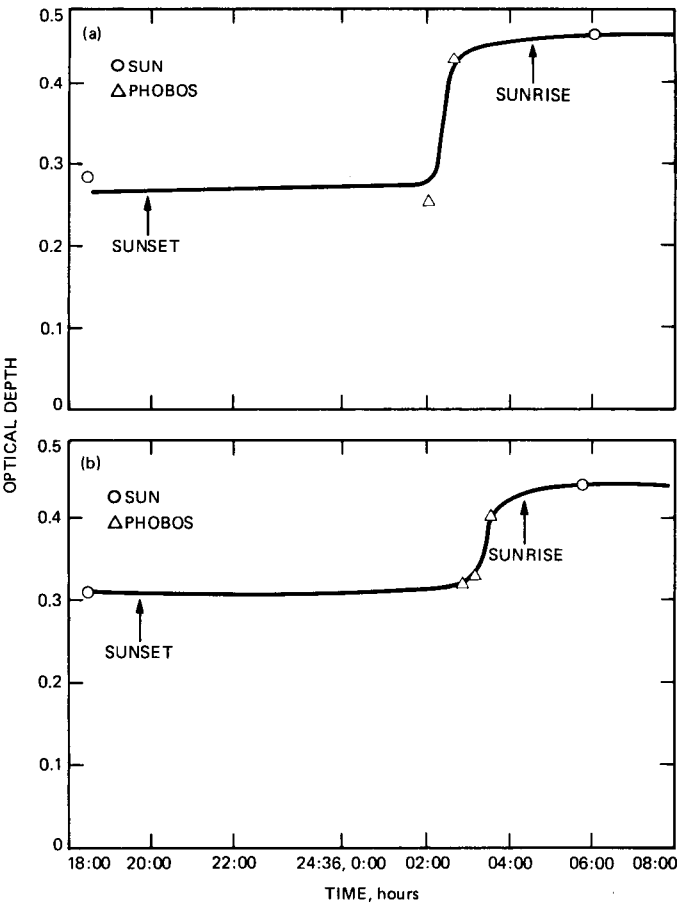

Fig. 5. Variation of optical depth (a) from the late afternoon of sol 24 to the early morning of sol 25 at the Viking Lander 2 site, as inferred from photograph of Phobos (triangles) and the sun (circles); (b) similar data from the late afternoon of sol 28 to the early morning of sol 29